

## Detection of Insulin-Like Growth Factor 1 Based on an Electrochemical Impedance Spectroscopy Sensor

Lin Ding<sup>1</sup>, Hongtao Zhang<sup>2,\*</sup>

<sup>1</sup> Department of Clinical Skills Experimental Teaching Center, Wuchang Hospital, Qiqihaer City, Heilongjiang Province, 161000, P.R. China

<sup>2</sup> Department of Obstetrics and Gynecology, Third Affiliated Hospital, Qiqihar Medical University, No.27, Tai Shun Street, Tiefeng District, Qiqihar City, Heilongjiang Province, 161000, P.R. China

\*E-mail: [hongtaozhang@126.com](mailto:hongtaozhang@126.com)

Received: 3 September 2017 / Accepted: 24 October 2017 / Published: 12 November 2017

---

This work presents the fabrication of a novel label-free electrochemical sensor towards the determination of insulin-like growth factor 1 (IGF-1) by immobilizing IGF-1 monoclonal antibodies using multiwalled carbon nanotubes (MWCNTs) and an ionic liquid (IL). It was found that the increased impedance values were linearly related with the logarithm of the IGF-1 concentrations (0.4 - 15 ng/mL). Furthermore, based on a signal-to-noise ratio of 3, the limit of detection (LOD) was calculated to be 22 pg/mL. The results showed that our developed sensor is highly stable, sensitive, and simple to use, showing potential for the early diagnosis of polycystic ovary syndrome.

---

**Keywords:** Insulin-like growth factor 1; Polycystic ovary syndrome; Multi-walled carbon nanotube; Electrochemical sensor; Ionic liquid

### 1. INTRODUCTION

Polycystic ovary syndrome (PCOS) is characterized by hyperandrogenism, amenorrhea, and anovulation [1-3], with obesity and insulin resistance usually observed [4]. In a polycystic ovary, folliculogenesis occurs in the early stages, and a preovulatory and dominant follicle cannot be selected, causing the small antral follicles to accumulate [5].

Normal ovarian cyclicity is known to be regulated by gonadotropins and intraovarian growth factor systems, and it has been assumed that abnormalities within the above systems might be an inducing factor for the pathogenesis of follicle maturation arrest in PCOS [6, 7]. The synthesis of androgens *in vitro* is stimulated by insulin-like growth factor I (IGF-I) and insulin acting on thecal-interstitial cells [8]. Increased IGF-I and insulin as well as LH has been assumed to result in the

clinically observed hyperandrogenaemia in PCOS through their action on *in vivo* thecal compartments [9, 10].

A configuration of binding proteins (IGFBPs) in circulation was used to modulate the *in vivo* actions of IGF-1. Six IGFBPs with homogeneous structures and distinct functionalities were measured and numbered based on the sequence of their identification. Among them, IGFBP-1 distinctively affects the dynamic regulation of the bioavailability of the serum IGF-I [11-13]. An inverse correlation was recorded between the serum IGFBP-1 and the free fraction estimation of IGF-I [14, 15]. Hence, IGF-I detection plays a vital role in practical PCOS diagnostics.

For the quantification of IGF-I, several strategies have been reported, including chromatography/electrospray ionisation tandem mass spectrometry [16, 17] and radioimmunoassay [18]. It has been known that electrochemical sensors should be highly selective, sensitive and easy to use, and they have gained substantial attention during the past decades [19-22]. Electrochemical impedance spectroscopy (EIS) measurements have been used for the direct detection of species, due to the electrochemical inertness of most biological molecules [23-28]. The EIS strategy is more cost-effective than other methods due to the requirement of no additional materials such as labelled antibodies. In addition, EIS is non-destructive and could be used to investigate the electrical features of biological interfaces [29, 30]. Therefore, the use of EIS has increased in many biological fields [31-33].

In the present work, IGF-I was sensitively determined using a new electrochemical impedance sensor prepared based on MWCNTs and IL. The variation in impedance values was recorded to investigate the IGF-I concentration. Due to the large numbers of conducting microcavities provided by the MWCNTs and IL, our proposed sensor was exceptionally sensitive. Furthermore, this sensor was label free, low cost, and easy to use. Therefore, our proposed sensor has a great potential to be used for the early diagnostics of PCOS.

## 2. EXPERIMENTS

### 2.1. Chemicals

The monoclonal anti-human IGF-1 antibody (primary antibody) and the receptor grade IGF-1 were provided by immunological & biochemical test systems GmbH (Reutlingen, Germany). A 10 mM phosphate buffer solution (PBS), pH 7.5, consisted of KCl (2.7 mM), NaCl (137 mM),  $\text{KH}_2\text{PO}_4$  (14 mM), and  $\text{Na}_2\text{HPO}_4$  (87 mM). For the preparation of the electrochemical probes, the supporting electrolyte (0.1 M KCl) was mixed with an aqueous solution (1.0 mM) of  $\text{K}_4\text{Fe}(\text{CN})_6$  and  $\text{K}_3\text{Fe}(\text{CN})_6$  (1:1). 1-Butyl-3-methylimidazolium hexafluorophosphate ( $[\text{bmim}]\text{PF}_6$ ) was commercially available from Hangzhou Kemer Chemical Co., Ltd. (China). The 95% multiwalled carbon nanotubes (MWCNTs) with a length of 1 to 2  $\mu\text{m}$  and a diameter of 10 to 20 nm were commercially available from Shenzhen Nanotech Port Co., Ltd.

## 2.2. Functionalization of MWCNTs

After suspending in a concentrated nitric/sulfuric acid mixture (3:1 v/v), the MWCNTs were sonicated for 16 h. Subsequently, the as-prepared MWCNTs were filtered to yield shortened carboxylate MWCNTs (SC-MWCNTs), followed by thoroughly rinsing with water.

## 2.3. Electrodes preparation

The glassy carbon electrodes (GCE) with diameters of 3 mm were polished to a mirror-like appearance using alumina powder (0.3 and 0.05  $\mu\text{m}$ ) before modification. After successive sonication in 1:1 nitric acid/water solution (v/v), acetone, and ultrapure water, the as-prepared electrodes were left drying under a nitrogen stream. For the preparation of the MWCNTs/ionic liquid (MWCNT/IL), the IL was mixed with the as-prepared SC-MWCNTs (0.5 mg) and ground using an agate mortar for *ca.* 60 min. The obtained suspensions were subsequently centrifuged at 15,000 rpm for *ca.* 0.5 h. Using a pipette, the supernatant was removed to yield the [bmim]PF<sub>6</sub>/MWCNTs. The MWCNT/IL/GCE was prepared by dropping Ab solution (0.25 mL) onto the as-prepared MWCNT/IL mixture, followed by gentle stirring for 30 min. The electrochemical biosensing layers were formed on the surface of the electrode after dropping the as-prepared mixture (3  $\mu\text{L}$ ). This was followed by drying the electrodes in a fume cupboard at ambient temperature for 8 h. The sensor immunity was guaranteed by incubating the electrodes in pH 7.5 PBS (10 mL) + IGF-1 of varying concentrations at 37 °C for 25 min. The as-prepared MWCNT/IL/Ab/AFB<sub>1</sub>/GCE was successively rinsed with water and pH 7.5 phosphate-buffered saline solutions. For comparison, the MWCNT/IL/GCE was fabricated in a comparable way. Prior to use, the as-prepared immunosensor was stored at 4 °C and denoted IGF-1/Ab/MWCNT/IL/GCE.

## 2.4. Immunoassay measurement

A CHI 660D electrochemical workstation (CH Instruments, Shanghai, China) was used for all electrochemical measurements. A traditional three-electrode configuration was used consisting of a bare or modified GCE as the working electrode, a saturated calomel electrode (SCE) as the reference electrode, and a platinum wire as the auxiliary electrode. The cyclic voltammetry (CV) and EIS measurements were performed in PBS solution containing K<sub>3</sub>[Fe(CN)<sub>6</sub>]/K<sub>4</sub>[Fe(CN)<sub>6</sub>] (5.0 mM) and KCl (0.1 M), and the scan rate was 100 mV/s. For the EIS experiment, the sine wave potential showed an amplitude of 10 mV, and the frequency ranged from 10<sup>-1</sup> to 10<sup>5</sup> Hz.

## 3. RESULTS AND DISCUSSION

The electrode performance after each assembly step was studied using CV measurement. As shown in Fig. 1, Fe(CN)<sub>6</sub><sup>3-/4-</sup> was characterized via CV using the bare GCE, MWCNT/IL-modified GCE, Ab/MWCNT/IL-modified GCE, and IGF-1/Ab/MWCNT/IL-modified GCE, respectively. As the

electrode was modified stepwise, a gradual reduction in the redox current was observed (Fig. 1), which indicated that electron transfer was blocked between the electrode surface and the  $\text{Fe}(\text{CN})_6^{3-/4-}$  probe. These changes are attributed to an increased interfacial concentration of the anionic probe ( $[\text{Fe}(\text{CN})_6]^{3-/4-}$ ) due to its strong affinity to the polycationic ( $\text{NH}_3^+$ ) layer of the amino groups of the BSA [34]. Obviously, electron transfer was significantly inhibited after the immobilization of Ab, which suggests that the cathodic and anodic peak currents were remarkably diminished.

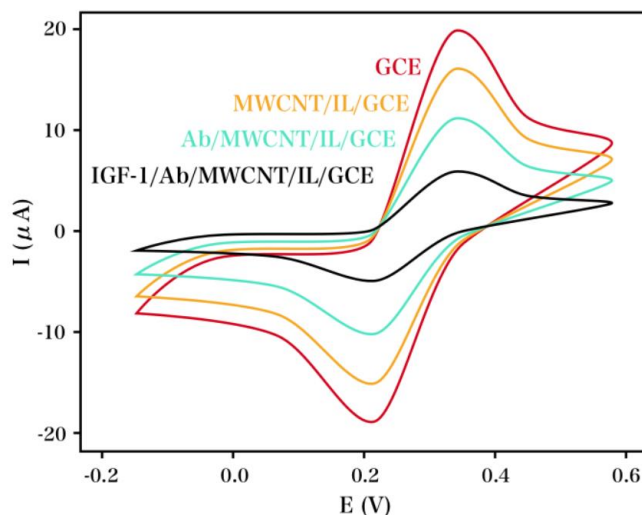


**Figure 1.** CVs recorded for  $\text{Fe}(\text{CN})_6^{3-/4-}$  using bare GCE, MWCNT/IL/GCE, Ab/MWCNT/IL/GCE, and IGF-1/Ab/MWCNT/IL/GCE.

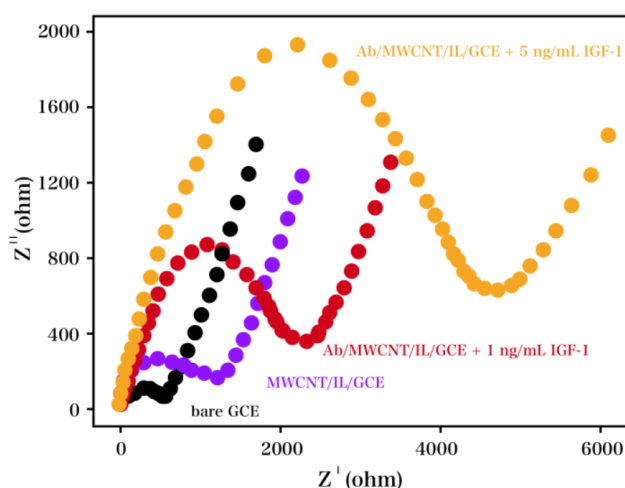


**Figure 2.** EIS patterns recorded for bare GCE, MWCNT/IL/GCE, and Ab/MWCNT/IL/GCE in pH 7.5 PBS + (1.0 ng/mL and 5.0 ng/mL) IGF-1 in the presence of 1.0 mM  $[\text{Fe}(\text{CN})_6]^{3-/4-}$  for 25 min.

Electrochemical impedance spectroscopy is a highly effective technique for investigating the electron-transfer properties of the modified electrodes [35, 36]. The EIS pattern consists of a semicircle section at high frequencies and a linear section at low frequencies, corresponding to an electron transfer limiting process and the diffusion limited step during the electrochemical process. The electron transfer resistance ( $R_{et}$ ) is inferred by the diameter of the semicircle [37]. The fitting of

the impedance data to  $R_{ct}$  was achieved using an equivalent circuit model, as shown in the inset of Fig. 2. The electron-transfer resistance for the redox process of the probe using bare GCE was *ca.* 150.7  $\Omega$ , whereas that for the Ab/MWCNT/IL-modified GCE was higher. The  $R_{ct}$  values were found to increase to 1844  $\Omega$  and 4179  $\Omega$  upon the immobilization of IGF-1 onto the Ab/MWCNT/IL-modified GCE, in proportion to the IGF-1 amount. Due to the interaction between Ab and IGF-1, electrically insulating bioconjugates were formed, blocking the electron-transfer process and leading to the  $R_{ct}$  increase. Hence, the results from the EIS and CV experiments were consistent with each other. In contrast, the linear portion coinciding with the diffusion limited electron shift occurred at comparatively lower frequencies. It can be proposed that the spectra were similar to those of Randle's equivalent circuit in theory [38, 39].

The result also indicated that  $R_{ct}$  is a suitable signal for sensing the interfacial properties of the prepared immunosensor during all of the modification steps. During the preparation of the modified film on an immunosensor, some parameters such as the incubation time of the antigen and the solution pH were associated with electrochemical signals. Non-Faradaic impedance biosensors perform impedance measurement in the absence of redox probes. Bacterial detection is based on the impedance change upon the attachment of bacterial cells on an interdigitated microelectrode in the absence of redox probes in the sample solution [40]. The protein activity has been found to significantly depend on the pH; thus, the pH was optimized herein. As the pH increased in a range of 6.0 - 8.0, an increase in  $\Delta R_{ct}$  was observed, as shown in Fig. 3A. When the pH was 7.5, a maximal response was recorded on the immunosensor; thus, pH 7.5 was used for the following experiments. The capturing of antigens on the surface of the electrode was significantly influenced by the incubation time. As shown in Fig. 3B, the Ab/MWCNT/IL-modified GCE showed an increased impedance response with prolonged incubation time in the presence of IGF-1 (7 ng/mL), and a plateau was reached after 25 min (Fig. 3B). This result suggested the saturating tendency of the bonding sites of the antibodies. On the other hand, the response was not enhanced with further increases in the incubation time, and therefore, 25 min was determined as the optimum incubation time for IGF-1.

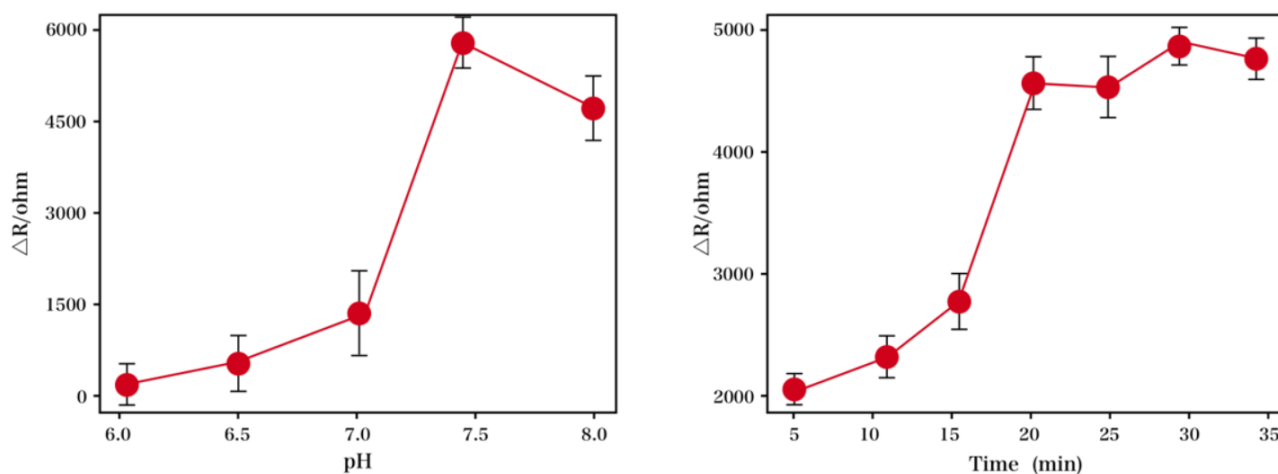


**Figure 3.** Influence of (A) the pH of PBS on the specific binding of IGF-1 and the Ab immobilized on the immunosensor surface. (B) The incubation time on the specific binding of IGF-1 and the antibodies immobilized on the immunosensor surface.

Fig. 4 presented the behaviour of our developed immunosensor towards the detection of varying concentrations of IGF-1. As the IGF-1 concentration was increased, an increase in the semicircle diameter was observed, as shown in the Nyquist plots of the impedance spectra in Fig. 4A. The  $R_{ct}$  variation was linearly related with the logarithm of IGF-1 (0.4 to 15 ng/mL), as shown in the calibration curve for IGF-1 in Fig. 4B. Based on a signal-to-noise ratio of 3, the LOD was obtained as 22 pg/mL. Table 1 presents the comparison of our developed sensor and other sensors proposed elsewhere.

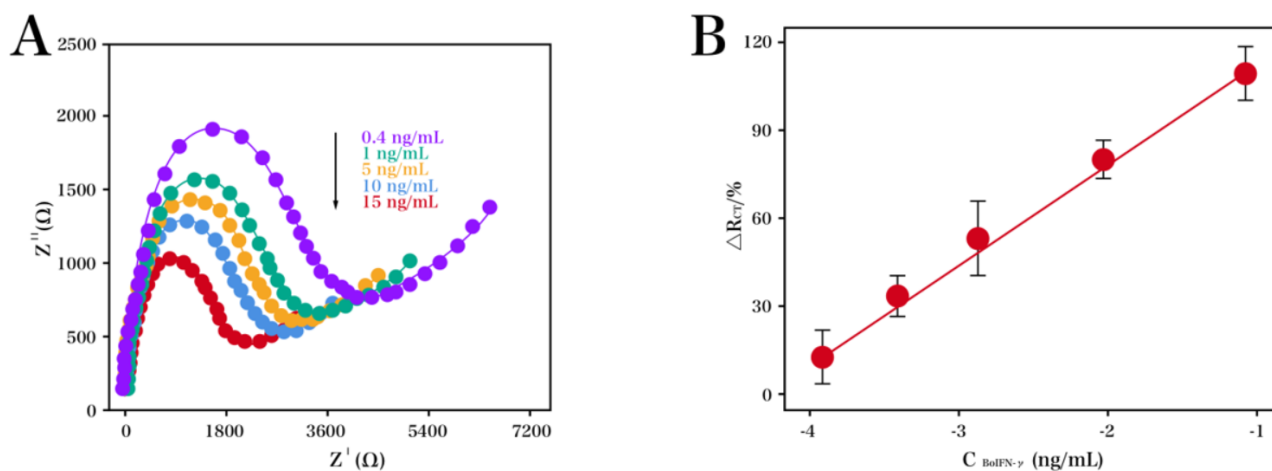


**Figure 4.** (A) Faradaic impedance spectra recorded for our proposed immunosensor incubated with IGF-1 (0.4, 1, 5, 10 and 15 ng/mL) in PBS solution. (B) Calibration curve recorded for IGF-1.

**Table 1.** Performance comparison of the Ab/MWCNT/IL modified GCE and other detection approaches towards IGF-1.

Method	Linear range	Detection limit	Reference
Liquid chromatography/electrospray ionisation tandem mass spectrometry	0.3-2 ng/mL	—	[16]
Mass spectrometry	1-40 ng/mL	—	[17]
IFN- $\gamma$ /BSA/anti-IFN- $\gamma$ /ZnO/GCE	0.0001-0.1 ng/mL	0.12 pg/mL	[41]
Ab/MWCNT/IL/GCE	0.4-15ng/mL	22 pg/mL	This work

EIS measurements were carried out to investigate the reproducibility of our developed immunosensor towards IGF-1. After six replicated experiments in the presence of IGF-1 (1 ng/mL), the EIS was obtained as 3.7%, which suggested that this sensor was highly reproducible. After experiments with six immunosensors prepared in six batches in the presence of IGF-1 (1 ng/mL), the EIS was obtained as 3.7%, which suggested that the preparation of this sensor was highly reproducible. In addition, no obvious change in the  $R_{ct}$  values was found after its storage at 4 °C in a refrigerator for 60 days, indicating the excellent microenvironment supplied by MWCNT for retaining the bioactivity of immobilized antibodies.

IGF-1 (0.5, 1, 5 and 10 ng/mL) was spiked into bovine serum specimens to study the accuracy and application potential of our proposed immunosensor towards the electrochemical detection of IGF-1. Table 2 presents the recovery results, which suggested that this sensor was exceptionally accurate in the label-free determination of IGF-1 in real specimens.

**Table 2.** Recoveries obtained for our developed immunosensor towards IGF-1 determination.

Sample	Added (ng/mL)	Found (ng/mL)	Recovery (%)	RSD (%)
1	0.5	0.492	98.4	2.66
2	1	1.044	104.4	2.05
3	5	5.021	100.42	1.07
4	10	9.841	98.41	4.19

#### 4. CONCLUSIONS

The present work reported a novel electrochemical impedance sensor towards the label-free determination of IGF-1 by immobilizing IGF-1 monoclonal antibodies onto a MWCNT/IL-modified GCE. This sensor was confirmed to be highly stable, reproducible, specific, sensitive, and easy to use, in addition to operating in a wide linear range. The recovery tests showed that our developed sensor was highly accurate and could be potentially applied to the determination of IGF-1 in real specimens.

#### ACKNOWLEDGEMENTS

This work was supported by grants from Science and Technology Project of Qiqihar, SFGG-201452.

#### References

- Messinis, C. Messini, G. Anifandis and K. Dafopoulos, *Best Practice & Research Clinical Obstetrics & Gynaecology*, 29 (2015) 479.
- B. Lee, I. Indran, H. Tan, Y. Li, Z. Zhang, J. Li and E. Yong, *Endocrinology*, 157 (2016) 382.
- A. Tokmak, M. Kokanali, A. Guzel, A. Kara, H. Topcu and S. Cavkaytar, *Asian Pac J Cancer Prev*, 15 (2014) 7011.
- M. Maliqueo, A. Benrick, A. Alvi, J. Johansson, M. Sun, F. Labrie, C. Ohlsson and E. Stener-Victorin, *Molecular and Cellular Endocrinology*, 412 (2015) 159.
- J. Hou, H. Cook-Andersen, H. Su, R. Shayya, K. Maas, C. Burt-Solorzano, A. Kumar and R. Chang, *Journal of Pediatric Endocrinology and Metabolism*, 29 (2016) 835.
- A. Nandi, Z. Chen, R. Patel and L. Poretsky, *Endocrinology and Metabolism Clinics of North America*, 43 (2014) 123.
- J. Rojas, M. Chávez, L. Olivar, M. Rojas, J. Morillo, J. Mejías, M. Calvo and V. Bermúdez, *International journal of reproductive medicine*, 2014 (2014)
- M. Ergenoglu, N. Yildirim, A. Yildirim, O. Yeniel, O. Erbas, A. Yavasoglu, D. Taskiran and N. Karadadas, *Reproductive Sciences*, 22 (2015) 942.
- D. Skubleny, N. Switzer, R. Gill, M. Dykstra, X. Shi, M. Sagle, C. de Gara, D. Birch and S. Karmali, *Obesity Surgery*, 26 (2016) 169.
- R. Simões, J. Soares-Jr, M. Simões, H. Nader, M. Baracat, G. Maciel, P. Serafini, R. Azziz and E. Baracat, *Journal of Ovarian Research*, 10 (2017) 54.
- C. Livingstone and A. Borai, *Clinical endocrinology*, 80 (2014) 773.
- N. Daan, M. Koster, R. Steegers-Theunissen, M. Eijkemans and B. Fauser, *Fertility and Sterility*, 107 (2017) 261.

13. A. Ciresi, M. Amato, J. Bianco and C. Giordano, *Journal of Pediatric Endocrinology and Metabolism*, 29 (2016) 571.
14. T. Piltonen, *Best Practice & Research Clinical Obstetrics & Gynaecology*, 37 (2016) 66.
15. N. Desai and S. Patel, *Gynecological Endocrinology*, 31 (2015) 801.
16. M. Bredehöft, W. Schänzer and M. Thevis, *Rapid Communications in Mass Spectrometry*, 22 (2008) 477.
17. N. Guha, D. Cowan, P. Sönksen and R. Holt, *Analytical and Bioanalytical Chemistry*, 405 (2013) 9669.
18. M. Kerr, A. Lee, P. Wang, K. Purushotham, N. Chegini, H. Yamamoto and M. Humphreys-Beher, *Biochemical Pharmacology*, 49 (1995) 1521.
19. Z. Wang, F. Li, J. Xia, L. Xia, F. Zhang, S. Bi, G. Shi, Y. Xia, J. Liu and Y. Li, *Biosensors and Bioelectronics*, 61 (2014) 391.
20. E. Paleček, J. Tkáč, M. Bartošík, T.s. Bertók, V. Ostatná and J. Paleček, *Chemical Reviews*, 115 (2015) 2045.
21. W. Song, H. Li, H. Liu, Z. Wu, W. Qiang and D. Xu, *Electrochemistry Communications*, 31 (2013) 16.
22. D. Bellin, H. Sakhtah, J. Rosenstein, P. Levine, J. Thimot, K. Emmett, L. Dietrich and K. Shepard, *Nature Communications*, 5 (2014) 3256.
23. M. MacDonald and H.A. Andreas, *Electrochimica Acta*, 129 (2014) 290.
24. D. Zhang, Y. Lu, Q. Zhang, L. Liu, S. Li, Y. Yao, J. Jiang, G.L. Liu and Q. Liu, *Sensors and Actuators B: Chemical*, 222 (2016) 994.
25. H. Chen, Q. Mei, S. Jia, K. Koh, K. Wang and X. Liu, *Analyst*, 139 (2014) 4476.
26. N. Formisano, P. Jolly, N. Bhalla, M. Cromhout, S. Flanagan, R. Fogel, J.L. Limson and P. Estrela, *Sensors and Actuators B: Chemical*, 220 (2015) 369.
27. J. Lazar, M. Bialon, C. Püttmann, C. Stein, W. Germeraad and U. Schnakenberg, *Lékař a technika-Clinician and Technology*, 45 (2015) 105.
28. Z. Guler and A. Sarac, *Express Polymer Letters*, 10 (2016) 96.
29. T. Pui, P. Kongsuphol, S. Arya and T. Bansal, *Sensors and Actuators B: Chemical*, 181 (2013) 494.
30. H. Wang, H. Zhang, S. Xu, T. Gan, K. Huang and Y. Liu, *Sensors and Actuators B: Chemical*, 194 (2014) 478.
31. Z. Taleat, C. Cristea, G. Marrazza, M. Mazloum-Ardakani and R. Săndulescu, *Journal of Electroanalytical Chemistry*, 717 (2014) 119.
32. B. Hong, A. Sun, L. Pang, A. Venkatesh, D. Hall and Y. Fainman, *Optics express*, 23 (2015) 30237.
33. W. Liang, S. Wang, F. Festa, P. Wiktor, W. Wang, M. Magee, J. LaBaer and N. Tao, *Analytical chemistry*, 86 (2014) 9860.
34. J. Zhao, C.R. Bradbury, S. Huclova, I. Potapova, M. Carrara and D.J. Fermín, *J Phys Chem B*, 109 (2005) 22985.
35. M. Grossi, G. Lecce, T. Toschi and B. Ricco, *IEEE Sensors Journal*, 14 (2016) 2947.
36. A. Biela, M. Watkinson, U. Meier, D. Baker, G. Giovannoni, C.R. Becer and S. Krause, *Biosensors & Bioelectronics*, 68 (2015) 660.
37. R. Cui, H. Huang, Z. Yin, D. Gao and J. Zhu, *Biosensors and Bioelectronics*, 23 (2008) 1666.
38. R. Chand, D. Han, S. Neethirajan and Y. Kim, *Sensors and Actuators B: Chemical*, 248 (2017) 973.
39. M. Huang, H. Li, H. He, X. Zhang and S. Wang, *Analytical Methods*, 8 (2016) 7413.
40. C. Conesa, C. Ibáñez, L. Seguí, P. Fito and N. Laguarda-Miró, *Sensors*, 16 (2016) 188.
41. L. Zhibo, (2017) 2389